

# Effect of Glycidyl Methacrylate-Grafted Natural Rubber on Physical Properties of Polylactic Acid and Natural Rubber Blends

Punmanee Juntuek,<sup>1,2</sup> Chaiwat Ruksakulpiwat,<sup>3</sup> Pranee Chumsamrong,<sup>1,2</sup>  
Yupaporn Ruksakulpiwat<sup>1,2</sup>

<sup>1</sup>School of Polymer Engineering, Institute of Engineering, Suranaree University of Technology,  
Nakhon Ratchasima 30000, Thailand

<sup>2</sup>Center for Petroleum, Petrochemical and Advanced materials, Chulalongkorn University, Bangkok 10330, Thailand

<sup>3</sup>Department of Chemistry, Faculty of Science, Khon Kaen University, Khon Kaen 40002, Thailand

Received 24 January 2011; accepted 29 September 2011

DOI 10.1002/app.36263

Published online 27 December 2011 in Wiley Online Library (wileyonlinelibrary.com).

**ABSTRACT:** Natural rubber (NR) was melt blended with polylactic acid (PLA) at various ratios using an internal mixer. The impact strength and elongation at break of PLA/NR blend dramatically increased with increasing NR content up to 10% (w/w). Glycidyl methacrylate-grafted natural rubber (NR-g-GMA) was used as a compatibilizer for PLA/NR blend. The effects of content and %grafting of NR-g-GMA on mechanical properties of PLA/NR blend were studied. The experimental result showed that the addition of NR-g-GMA in PLA/NR blend significantly improved impact strength and elongation at break of PLA/NR blend when compared with that of neat PLA

and PLA/NR blend without NR-g-GMA. The impact strength and elongation at break of PLA/NR blend increased with increasing NR-g-GMA content up to 1% (w/w). Moreover, with increasing % grafting of NR-g-GMA in PLA/NR blend up to 4.35, the impact strength and elongation at break of the blend increased. Morphological and thermal property of PLA, PLA/NR, and PLA/NR/NR-g-GMA were elucidated as well. © 2011 Wiley Periodicals, Inc. *J Appl Polym Sci* 125: 745–754, 2012

**Key words:** polylactic acid; natural rubber; polymer blend; reactive blending

## INTRODUCTION

Poly(lactic acid) (PLA) is a synthetic aliphatic polyester derived from biomass. Because of its renewability, biodegradability, and greenhouse gas neutrality, it has been emerging as an alternative to conventional petroleum-based polymeric materials. However, the inherent brittleness, low-melt viscosity, and low-heat distortion temperature of PLA led to its restricted applications.<sup>1</sup> To improve its property, it is now common practice to modify PLA by physical blending. For example, PLA was blended with other more flexible polymers such as polycaprolactone (PCL),<sup>2–4</sup> polybutylenesuccinate,<sup>5</sup> poly(butylene succinate-co-L-lactate),<sup>6</sup> and poly(butylene adipate-co-terephthalate).<sup>7,8</sup> In general, these blends showed considerably higher toughness than pure PLA. However, a significant decrease in tensile strength and modulus of the blends can be observed. As a consequence, the improvement of mechanical properties of PLA blends is still necessary to obtain material with optimum performance. Moreover, these flexible

polymers come from petroleum resource, whose price tends to increase in the future. Therefore, new material from renewable resource has received a lot of attention from researchers. Natural rubber (NR) is an interesting candidate to use as an impact modifier for PLA, because it has excellent properties such as high strength, high resilience, and high elongation at break.<sup>9</sup> NR has been used to improve mechanical properties of other polymers such as poly(ethylene terephthalate) (PET),<sup>10</sup> polystyrene,<sup>11</sup> and polypropylene (PP).<sup>12</sup> The improvement in impact strength of these polymers when adding NR was reported. However, Carvalho et al. found that the elongation at break of thermoplastic starch (TPS)/NR blend was increased when using NR content from 2.5 to 5% (w/w) and decreased when using higher NR content.<sup>13</sup> The difference in polarity of TPS and NR led to a phase separation and the blends became brittle at high NR content. The phase separation of NR blends due to the difference in polarity and molecular weight was also reported by several researchers.<sup>14–16</sup> In case of PLA/NR blend, the difference in the polarity and molecular weight of PLA and NR may result in the poor compatibility between PLA and NR. This may lead to the poor impact strength of PLA and NR blend. Thus, the compatibility between PLA and NR need to be

Correspondence to: Y. Ruksakulpiwat (yupa@sut.ac.th).

improved to obtain the blend with higher impact property. In general, there are two ways to improve compatibility of polymer blend. One is to induce a chemical reaction, leading to a modification of the polymer interface in two-phase blends. Another way is to add a third component called compatibilizer, which increases the interaction between immiscible phases. The third component can be block, homopolymer or graft copolymer, which can interact with both phases. The compatibilization of PLA blends has been extensively studied.<sup>17–19</sup> The elongation at break of the reactively compatibilized PLA/PCL blends was improved significantly when compared with that of pure PLA.<sup>20</sup> The compatibility of PLA/starch blends was improved using various compatibilizers such as maleic anhydride (MA)-grafted PLA (PLA-g-MA),<sup>21</sup> poly (L-lactide)-g-starch copolymer (PLLA-g-St),<sup>22</sup> and thermoplastic polyolefin elastomer-graft-poly lactide (TPO-PLA).<sup>23</sup> Glycidyl methacrylate (GMA)-grafted polymers such as styrene/acrylonitrile/glycidyl methacrylate copolymer (SAN-GMA)<sup>24</sup> and glycidyl methacrylate-grafted poly(ethylene octane) (GMA-g-POE)<sup>25</sup> are often used as compatibilizer for PLA blends. Oyama toughened PLA by reactive blending with poly (ethylene-glycidyl methacrylate; EGMA).<sup>26</sup> This study demonstrated a dramatic improvement in the mechanical characteristics of PLA by its reactive blending with EGMA. The elongation at break of PLA blends showed 40 times higher than that of neat PLA. Moreover, grafted copolymers of GMA were used as compatibilizer in other polyester blends such as PET/PP blend,<sup>27</sup> PCL/cellulose acetate (CA) blend,<sup>28</sup> and high-density polyethylene/PET blend.<sup>29</sup> It is usually believed that epoxy groups of GMA can react with carboxyl or hydroxyl groups of polyester. From our previous study, GMA was successfully grafted onto NR by emulsion polymerization to obtain glycidyl methacrylate-grafted natural rubber (NR-g-GMA).<sup>30</sup> When PLA was mixed with NR-g-GMA to form blends, it was expected that the epoxy group in NR-g-GMA can react with the carboxyl groups located at the PLA chain ends during melt-mixing. This should enhance compatibility between PLA and NR. Thus, the toughness of PLA/NR blend should be improved by using NR-g-GMA as a compatibilizer. The effect of NR-g-GMA on mechanical, thermal, and morphological properties of PLA/NR blends was elucidated in this study.

## EXPERIMENTAL

### Materials

Thai natural rubber (grade STR 5L) was purchased from Thaihua Latex. A commercial grade of PLA (PLA 4042D) was purchased from NatureWorks

**TABLE I**  
**Blend Compositions**

Symbols	PLA (wt %)	NR (wt %)	NR-g- GMA (wt %)
PLA	100	–	–
PLA/NR (95/5)	95	5	–
PLA/NR (90/10)	90	10	–
PLA/NR (85/15)	85	15	–
PLA/NR (80/20)	80	20	–
PLA/NR/NR-g-GMA (A) (90/9/1)	90	9	1
PLA/NR/NR-g-GMA (B) (90/9/1)	90	9	1
PLA/NR/NR-g-GMA (C) (90/9/1)	90	9	1
PLA/NR/NR-g-GMA (D) (90/9/1)	90	9	1
PLA/NR/NR-g-GMA (B) (90/9.8/0.2)	90	9.8	0.2
PLA/NR/NR-g-GMA (B) (90/7/3)	90	7	3
PLA/NR/NR-g-GMA (B) (90/5/5)	90	5	5

LLC. NR-g-GMA at various % grafting was prepared in our laboratory. The synthesis and characterization of NR-g-GMA including the calculation to find the % grafting of GMA monomer were given in details in our previous publication.<sup>30</sup> NR-g-GMA at various % grafting including 0.76, 4.35, 8.40, and 16.70 were used in this study and they were denoted by NR-g-GMA (A), NR-g-GMA (B), NR-g-GMA (C), and NR-g-GMA (D) respectively.

### Blends preparation

PLA blends were prepared using an internal mixer (Hakke Rheomix, 3000p) at the temperature of 170°C with a rotor speed of 60 rpm for 10 min. Before mixing, PLA was dried in an oven at 70°C for 4 h to eliminate moisture. The compositions of all blends are shown in Table I. After mixing in an internal mixer, the blend specimens were prepared by compression molding (LabTech, LP20-B) at melting temperature of 165°C and mold temperature of 25°C for subsequent measurements.

### Characterization

#### Thermal property

Thermogravimetric analysis (TGA) was performed using a TA Instrument thermo gravimetric analyzer (TGA, Mettler Toledo model TGA/DSC 1) by heating the sample from room temperature to 600°C at a heating rate of 20°C/min under a nitrogen atmosphere. The sample with a weight between 5 and 10 mg was used for each run.

#### Morphological property

The morphologies of the impact fractured surface and tensile fractured surface of compression molded samples were examined using a scanning electron

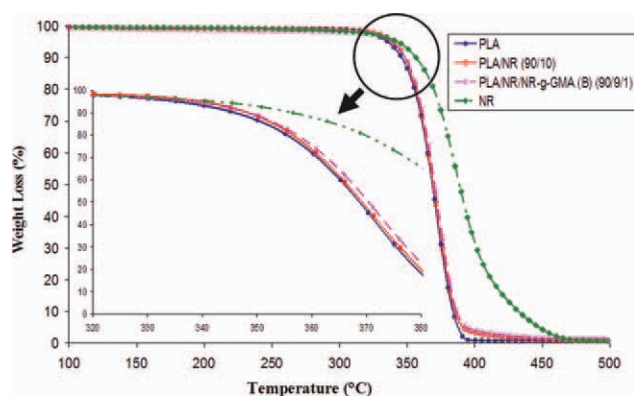


**Figure 1** TGA curves of PLA, PLA/NR (90/10), PLA/NR/NR-g-GMA (B) (90/9/1), and NR. [Color figure can be viewed in the online issue, which is available at [wileyonlinelibrary.com](http://wileyonlinelibrary.com).]

microscope (SEM, model JSM 5900LV). The specimens were coated with gold prior to the examination. Acceleration voltage of 10 kV was used to collect SEM images of the samples.

#### Mechanical properties

The unnotched Izod impact test was performed according to ASTM D256 using an Atlas testing machine (model BPI). Tensile properties were obtained according to ASTM D638 using an Instron universal testing machine (UTM, model 5565) with a load cell of 5 kN.

#### Interaction of PLA and NR-g-GMA

PLA was melt blended with NR-g-GMA(C) using an internal mixer (Hakke Rheomix, 3000p) at the temperature of 170°C with a rotor speed of 60 rpm for 10 min. The interaction between PLA and NR-g-GMA(C) blend [PLA/NR-g-GMA(C)] was evaluated using Fourier transform infrared (FT-IR) spectrometer (Spectrum one). The spectra were obtained at 4  $\text{cm}^{-1}$  resolution in the wave number range from 4000 to 650  $\text{cm}^{-1}$ . The FT-IR samples were prepared by casting polymer films. All samples were dried in an oven at 70°C for 24 h before testing.

## RESULTS AND DISCUSSION

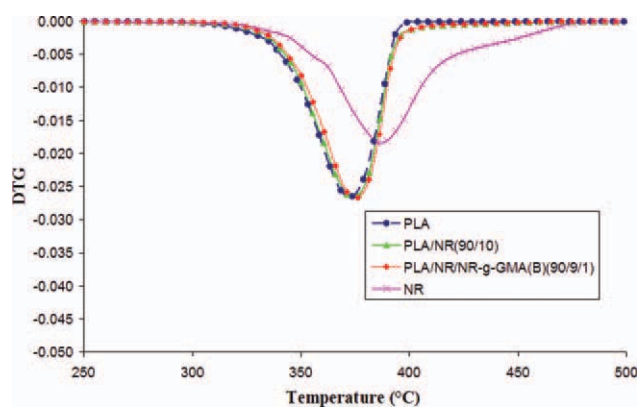
### Thermal properties of PLA, NR, PLA/NR, and PLA/NR/NR-g-GMA

TGA and DTG curves of PLA, PLA/NR (90/10), PLA/NR/NR-g-GMA (B) (90/9/1), and NR are shown in Figures 1 and 2, respectively. It is evident that the thermal degradation of PLA and NR showed only single step of weight loss. The onset degradation temperatures of PLA and NR were 290.76 and 305.33°C, respectively. The final degrada-

tion temperature of PLA and NR were noticed at 409.67 and 490.62°C, respectively. This indicated the higher thermal stability of NR when compared with that of PLA. The onset degradation temperature of PLA/NR (90/10) was 294.20°C, which is about 4°C higher than PLA. The slight increase in thermal stability of PLA/NR (90/10) has been attributed to the higher thermal stability of NR. Moreover, PLA/NR/NR-g-GMA (B) (90/9/1) showed higher onset degradation temperatures (301.59°C) than that of PLA/NR (90/10). The increase in thermal stability of PLA/NR when using NR-g-GMA as compatibilizer might be attributed to the higher interaction and better dispersion of NR in PLA matrix. An increase in thermal stability of PLA due to the good interaction between the blend components was also reported in other PLA blends and composites. Girija et al. studied thermal properties of polyethylene terephthalate (PET) and PLA blend. They found that thermal stability of PLA was increased by the addition of PET to PLA.<sup>31</sup> Moreover, Feijoo et al. found that the thermal stability of PLA composite was increased when the interaction and dispersion of the components were improved.<sup>32</sup>

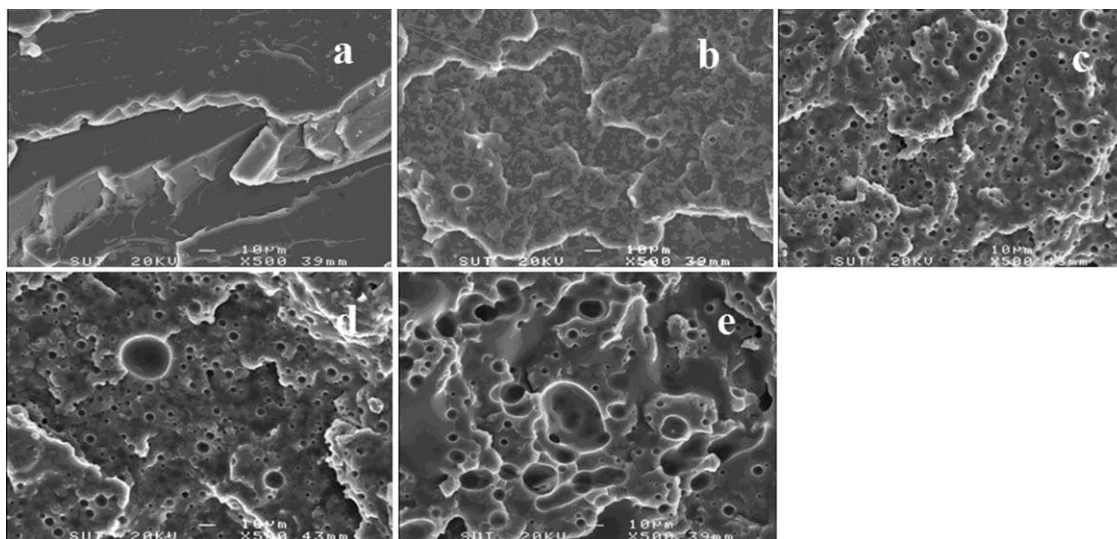
### Effect of NR content on morphological and mechanical properties of PLA/NR blend

Figure 3(a–e) shows SEM micrographs of impact fractured surface of PLA and PLA/NR blends with increasing NR contents from 5 to 20% (w/w). The micrographs of the blends showed two phases with irregular domain size and shape. This indicates that PLA/NR blends are completely immiscible, where NR domains are dispersed in PLA matrix. When 10% (w/w) NR was added, the domain size of NR was about 5–10  $\mu\text{m}$  [as shown in Fig. 3(c)]. In case of PLA/NR (80/15 and 80/20), the average domain size of NR was much larger than 10  $\mu\text{m}$  [Fig. 3(d,e)].



**Figure 2** DTG curves of PLA, PLA/NR (90/10), PLA/NR/NR-g-GMA (B) (90/9/1), and NR. [Color figure can be viewed in the online issue, which is available at [wileyonlinelibrary.com](http://wileyonlinelibrary.com).]





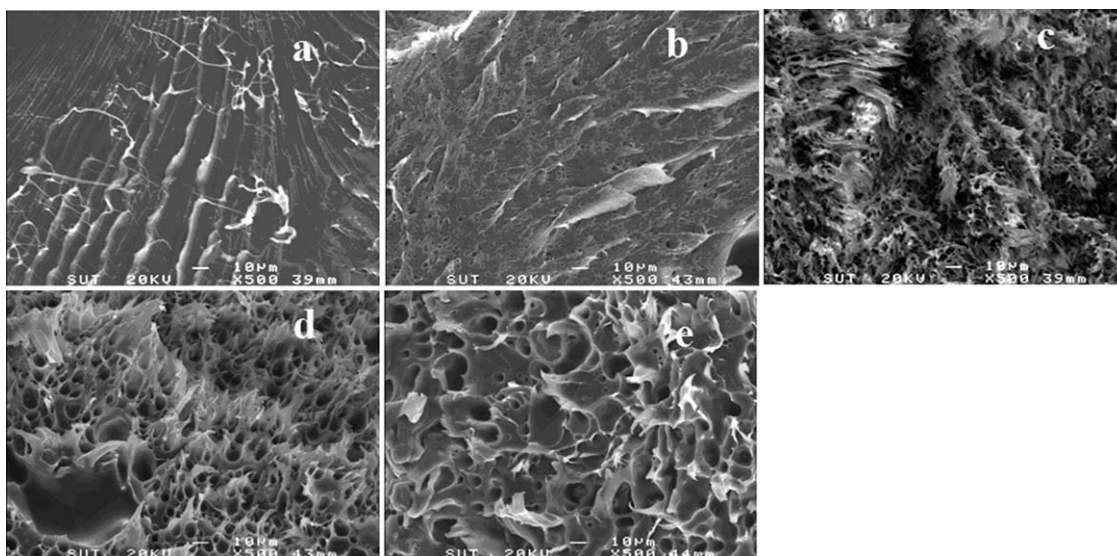
**Figure 3** SEM micrographs of impact fractured surface of PLA (a), PLA/NR (95/5) (b), PLA/NR (90/10) (c), PLA/NR (80/15) (d), and PLA/NR (80/20) (e).

This implied that the coagulation of NR phase appeared at high NR content. In general, in an immiscible blend system especially at high content of dispersed phase, polymers always coagulate individually due to their different chemical structures and high molecular weights.<sup>33</sup> Figure 4(a–e) shows SEM micrographs of tensile fractured surface of PLA and PLA/NR blends with increasing NR contents from 5 to 20% (w/w). For PLA/NR, more and longer fibrils can be observed from the surfaces when using NR content of 5 and 10% (w/w) as shown in Figure 4(b,c). This can be used as an evidence of ductile fractures. With increasing NR content to 15 and 20% (w/w) [Fig. 4(d,e)], the fibrils were longer than those

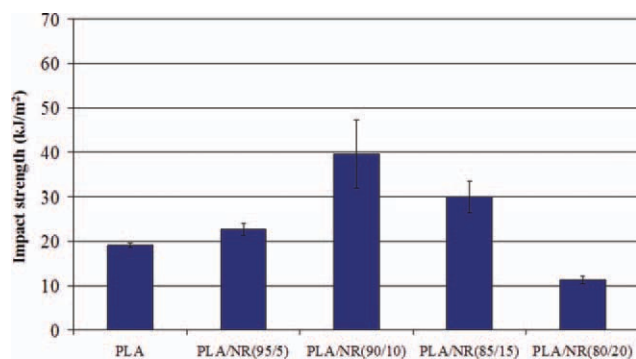
of samples with NR content of 5 and 10 % (w/w). However, the big oval cavities are visible. These cavities were formed during tension when NR was debonded from PLA matrix at the interface.

Figure 5 shows the impact strength of PLA, PLA/NR blends at various NR contents.

The impact strength of neat PLA was 19.06 kJ/m<sup>2</sup>. Impact strength of PLA/NR blends increased with increasing NR content up to 10% (w/w). When the NR content reached 10% (w/w), impact strength of the PLA/NR blend was 39.52 kJ/m<sup>2</sup>, which is about two times higher than that of neat PLA. However, when NR content was increased to 15% (w/w), impact strength of PLA/NR blend was decreased to



**Figure 4** SEM micrographs of tensile fractured surface of PLA (a), PLA/NR (95/5) (b), PLA/NR (90/10) (c), PLA/NR (80/15) (d), and PLA/NR (80/20) (e).



**Figure 5** Impact strength of PLA, PLA/NR blends at various NR contents. [Color figure can be viewed in the online issue, which is available at [wileyonlinelibrary.com](http://wileyonlinelibrary.com).]

29.98 kJ/m<sup>2</sup>, but it was still higher than that of neat PLA. With further increased NR content to 20% (w/w), impact strength of PLA/NR blend was decreased to 11.26 kJ/m<sup>2</sup>, which was lower than that of neat PLA. This suggests that the optimum content of NR in PLA is 10% (w/w). Tensile strength, modulus, and elongation at break of PLA and PLA/NR blends at various NR contents are shown in Table II. Modulus and tensile strength of PLA/NR decreased with increasing NR content. The reduction in these mechanical properties was due to the result of the rubbery nature of NR. This behavior was also found in NR blend with other polymers such as nylon 6 (PA6).<sup>15</sup> Elongation at break was increased from 10.84% for neat PLA to 74.51% for PLA/NR (90/10). With increasing NR content to 15% and 20% (w/w), elongation at break of PLA/NR blends was decreased. There are many factors concerning with the effectiveness of rubber toughened polymer such as interfacial adhesion between rubber particles and matrix, type and concentration of rubber, blending method, processing conditions, and rubber particle size and shape. It is generally accepted that rubber particle size and interfacial adhesion between blend components take the key role in determining the mechanical performance of a polymer blend. For

example, a large particle size and weak adhesion would result in poor mechanical properties in the blends.<sup>34</sup> The decrease in elongation at break and impact strength of PLA/NR blends at high NR content might be due to the enlargement of the dispersed NR caused by the coagulation of NR phase as previously shown in SEM micrographs. Stress concentration usually takes place in the vicinity of the dispersed phase due to the difference of elastic modulus between the dispersed phases (NR) and the surrounding matrix (PLA), and initiates localized microdamages in this region resulting in the reduction of mechanical properties such as strength and toughness at high NR content. This behavior was also observed in the PLA/PCL blends.<sup>34</sup>

#### Effect of NR-g-GMA content on morphological and mechanical properties of PLA/NR blend

To study the effect of NR-g-GMA content and % grafting on morphological and mechanical properties of PLA/NR blends, PLA content was fixed at 90 wt % according to the highest impact strength of PLA/NR (90/10). The rest portion (10 wt %) was NR and NR-g-GMA. The ratio of NR to NR-g-GMA was varied (9.8/0.2, 9/1, 7/3, 5/5 wt %) as shown in Table I. Figure 6(a–e) shows SEM micrographs of impact fractured surface of PLA/NR blends containing 0.2–5% (w/w) of NR-g-GMA. The % grafting was fixed at 4.35. When 1% (w/w) of NR-g-GMA was added, the domain sizes of NR [as shown in Fig. 6(c)] were much smaller than that of PLA/NR (90/10) without NR-g-GMA [Fig. 6(a)]. This indicated that the compatibility between PLA and NR was improved when NR-g-GMA was used as compatibilizer. The interaction between PLA and NR-g-GMA(C) was investigated by FT-IR spectroscopy as shown in Figure 7. PLA shows a band centered at about 3500 cm<sup>-1</sup> in the hydroxyl-stretching region, which attributed to the end carboxyl group of PLA. When PLA was mixed with NR-g-GMA to form blends, the peak at

**TABLE II**  
Tensile Strength, Modulus, and Elongation at Break of PLA and PLA/NR Blends, and PLA/NR/NR-g-GMA

Samples	Tensile strength (MPa)	Elongation at break (%)	Modulus (GPa)
PLA	52.99 ± 0.65	10.84 ± 1.64	0.63 ± 0.04
PLA/NR (95/5)	41.04 ± 1.60	25.75 ± 4.79	0.62 ± 0.02
PLA/NR(90/10)	29.66 ± 1.56	74.51 ± 9.06	0.51 ± 0.04
PLA/NR(85/15)	28.91 ± 0.89	23.39 ± 1.59	0.50 ± 0.02
PLA/NR(80/20)	18.23 ± 1.28	7.43 ± 0.30	0.36 ± 0.02
PLA/NR/NR-g-GMA(B) (90/9.8/0.2)	29.70 ± 0.78	87.34 ± 7.88	0.51 ± 0.03
PLA/NR/NR-g-GMA (B) (90/9/1)	27.46 ± 0.66	159.08 ± 21.27	0.53 ± 0.02
PLA/NR/NR-g-GMA (B) (90/7/3)	26.65 ± 0.59	110.18 ± 18.46	0.51 ± 0.02
PLA/NR/NR-g-GMA (B) (90/5/5)	26.53 ± 0.98	88.14 ± 7.91	0.52 ± 0.05
PLA/NR/NR-g-GMA(A)(90/9/1)	27.41 ± 0.70	82.09 ± 10.00	0.51 ± 0.10
PLA/NR/NR-g-GMA(C)(90/9/1)	28.53 ± 1.68	86.79 ± 18.87	0.50 ± 0.06
PLA/NR/NR-g-GMA(D)(90/9/1)	29.49 ± 1.95	52.35 ± 6.74	0.51 ± 0.03

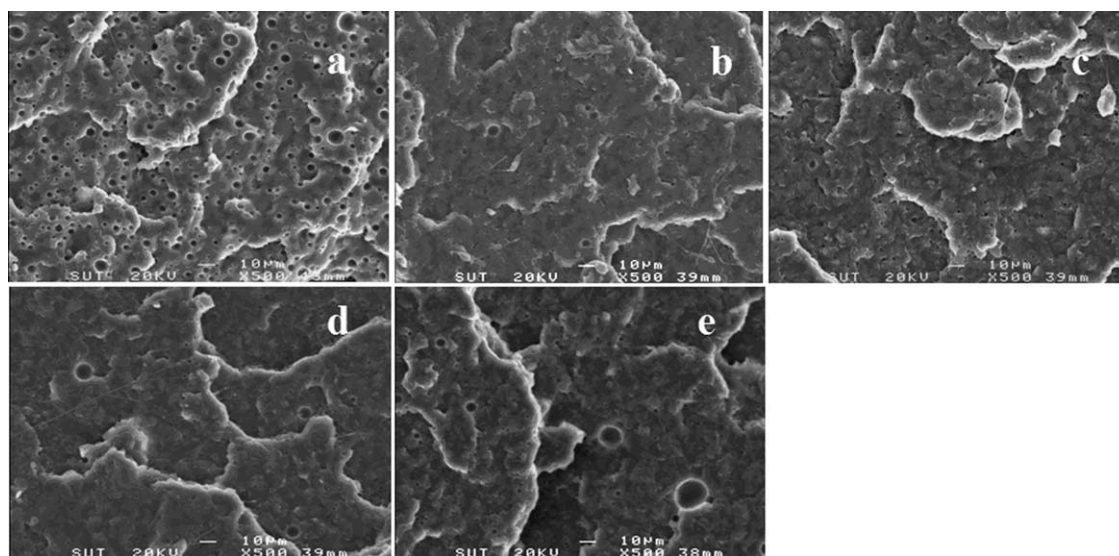


**Figure 6** SEM micrographs of impact fractured surface of PLA/NR (90/10) (a), PLA/NR/ NR-g-GMA (B) (90/9.8/0.2) (b), PLA/NR/NR-g-GMA (B) (90/9/1) (c), PLA/NR/NR-g-GMA (B) (90/7/3) (d), and PLA/NR/ NR-g-GMA (B) (90/5/5) (e).

$3500\text{ cm}^{-1}$  disappears. This can be considered that the epoxy group in NR-g-GMA reacted with the carboxyl groups located at the PLA chain ends during melt-mixing. This results in the improvement of

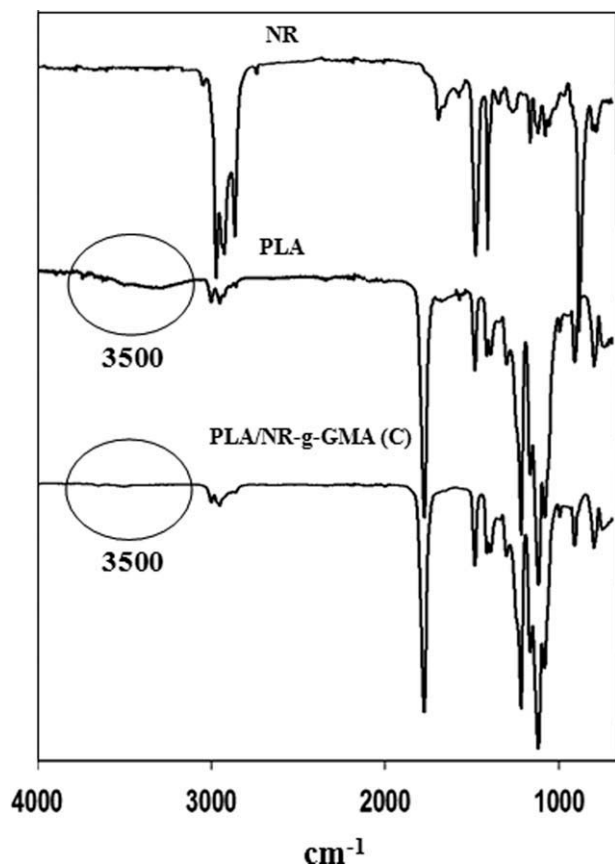


**Figure 7** FT-IR spectra of NR, PLA and PLA/NR-g-GMA(C) blend.

compatibility between PLA and NR. However, some large domain size of NR was appeared when NR-g-GMA content was increased to 3 and 5% (w/w). This may be attributed to the formation of a third phase in the system at high NR-g-GMA content. Figure 8(a–e) shows the tensile fractured surface of PLA/NR blends with NR-g-GMA contents of 0.2–5% (w/w). It was observed that the elongated fibrils of PLA/NR blend with NR-g-GMA were longer than that of PLA/NR blend without NR-g-GMA. This confirms that the addition of NR-g-GMA improved toughness of PLA/NR blend.

Figure 9 shows the impact strength of PLA, PLA/NR blends at various NR-g-GMA contents. The impact strength of PLA/NR blends increased dramatically with increasing NR-g-GMA content to 1% (w/w). The impact strength of PLA/NR blend with NR-g-GMA content of 1% was  $54.24\text{ kJ/m}^2$ , which is about 2.5 times higher than that of neat PLA. In contrast, the impact strength of PLA/NR blends without NR-g-GMA was only about two times higher than that of neat PLA. This is the result from an improvement in compatibility between PLA and NR via reactive blending as explained earlier. With increasing NR-g-GMA content to 3 and 5% (w/w), impact strength of PLA/NR blends was slightly decreased to  $51.34$  and  $49.27\text{ kJ/m}^2$ , respectively. However, these values were still higher than that of neat PLA and PLA/NR blend without NR-g-GMA. Tensile stress–strain curves of neat PLA and PLA blends are shown in Figure 10. The result showed that type of fracture of neat PLA is brittle fracture. PLA/NR blend exhibited plastic flow and higher elongation at break when compared with that of neat PLA. This indicated that PLA/NR blend was



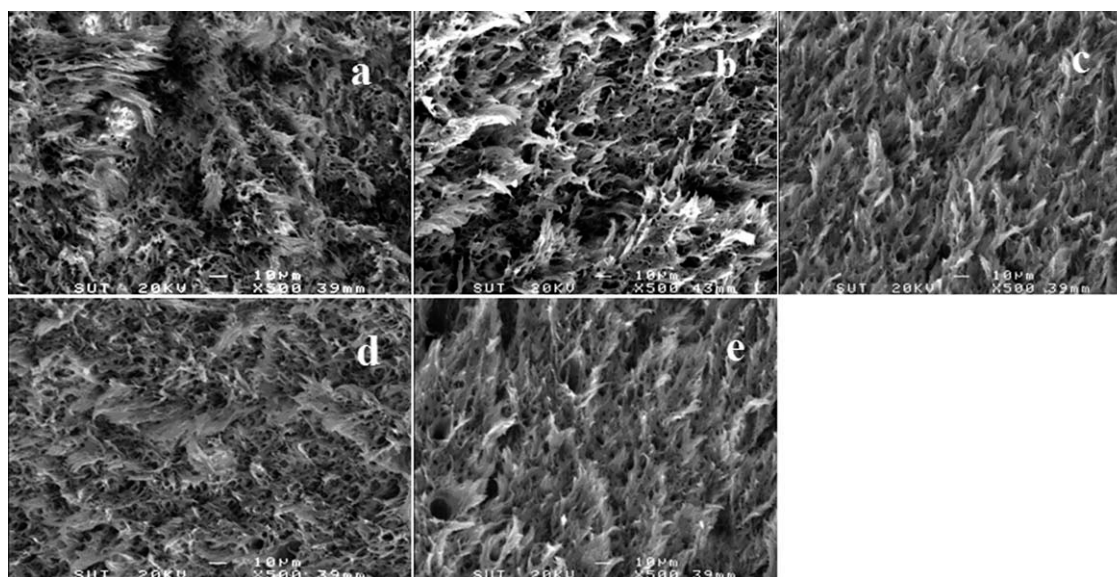


**Figure 8** SEM micrographs of tensile fractured surface of PLA/NR (90/10) (a), PLA/NR/ NR-g-GMA (B) (90/9.8/0.2) (b), PLA/NR/NR-g-GMA (B) (90/9/1) (c), PLA/NR/NR-g-GMA (B) (90/7/3) (d), and PLA/NR/ NR-g-GMA (B) (90/5/5) (e).

soft and ductile. Effects of NR-g-GMA content on mechanical properties of PLA/NR blend are illustrated in Table II. Elongation at break PLA/NR blend increased up to 159.08% with increasing NR-g-GMA content up to 1% (w/w), which is two times higher than that of PLA/NR blend without NR-g-GMA (74.51%). The ductility of this material was clearly much higher than that of neat PLA and PLA/NR blends without NR-g-GMA. Elongation at break of PLA/NR blends decreased with increasing NR-g-GMA content to 3 and 5% (w/w). However, it was still higher than PLA/NR blend without NR-g-GMA. Tensile strength of PLA/NR blends slightly decreased with increasing NR-g-GMA content, while the modulus insignificantly change when compared with PLA/NR blend without NR-g-GMA. The

decrease in tensile strength and elongation at break of PLA/NR at high NR-g-GMA content might be because of the appearance of some large domain size as previously shown by SEM micrographs.

#### Effect of % grafting of NR-g-GMA on morphological and mechanical properties of PLA/NR blend

Figure 11(a–e) shows SEM micrographs of impact fractured surface of PLA/NR with increasing % grafting of NR-g-GMA from 0.76 to 16.7. The domain sizes of NR at % grafting of 4.35 [Fig. 11(c)] were much smaller than that of PLA/NR (90/10) [Fig. 10(a)]. However, at % grafting of 8.4 and 16.7

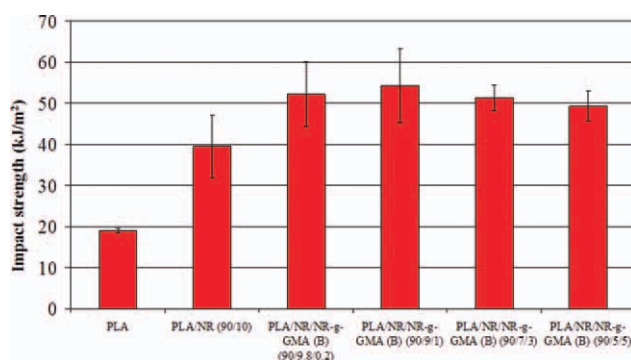


**Figure 9** Impact strength of PLA, PLA/NR(90/10) and PLA/NR/NR-g-GMA at various NR-g-GMA content. [Color figure can be viewed in the online issue, which is available at [wileyonlinelibrary.com](http://wileyonlinelibrary.com).]

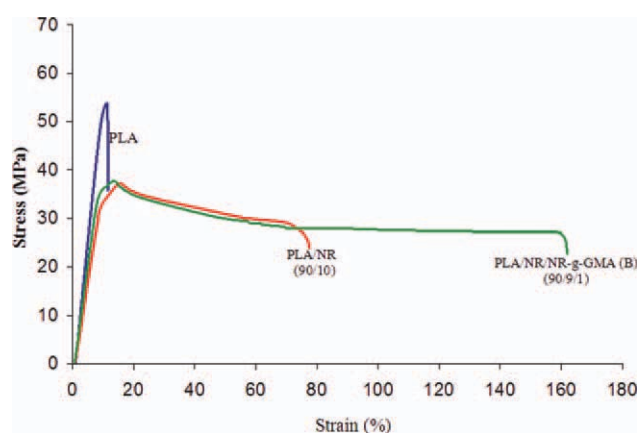


**Figure 10** Tensile stress–strain curves of PLA, PLA/NR (90/10) and PLA/NR/NR-g-GMA (B) (90/9/1). [Color figure can be viewed in the online issue, which is available at [wileyonlinelibrary.com](http://wileyonlinelibrary.com).]

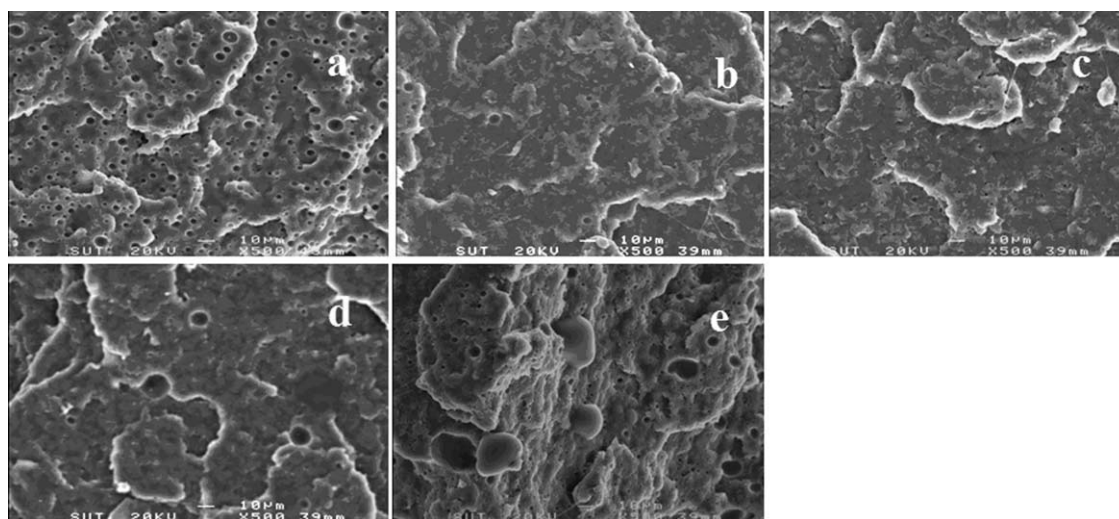


**Figure 11** SEM micrographs of impact fractured surface of PLA/NR (90/10) (a), PLA/NR/NR-g-GMA(A) (90/9/1) (b), PLA/NR/NR-g-GMA (B) (90/9/1) (c), PLA/NR/NR-g-GMA (C) (90/9/1) (d), and PLA/NR/NR-g-GMA (D) (90/9/1) (e).

[Fig. 11(d,e)], the domain sizes of NR were larger than that of at % grafting of 4.35 [Fig. 11(c)]. Tensile fractured surface of PLA/NR blends with increasing % grafting of NR-g-GMA is shown in Figure 12(a–e). The big oval cavities due to the debonding of NR particles from PLA matrix can be observed at high % grafting of NR-g-GMA (% grafting 8.4 and 16.7). Moreover, the elongated fibrils of PLA/NR blend with NR-g-GMA at high % grafting were shorter than those of PLA/NR blend with NR-g-GMA at low % grafting (grafting percentage 0.76 and 4.35). Polyglycidyl methacrylate is a hard and brittle poly-

mer. By grafting GMA onto NR, the hardness of NR was increased. This is due to the restriction of molecular chain movement of NR caused by GMA. Moreover, our previous study found that the hardness of NR-g-GMA increased with increasing % grafting of NR-g-GMA.<sup>30</sup> This made it difficult to disperse in PLA matrix at this mixing condition, so the large domain sizes of NR occurred at high % grafting of NR-g-GMA.

The impact strength of PLA, PLA/NR blends with NR-g-GMA at various percentages of grafting is shown in Figure 13. Impact strength of PLA/NR

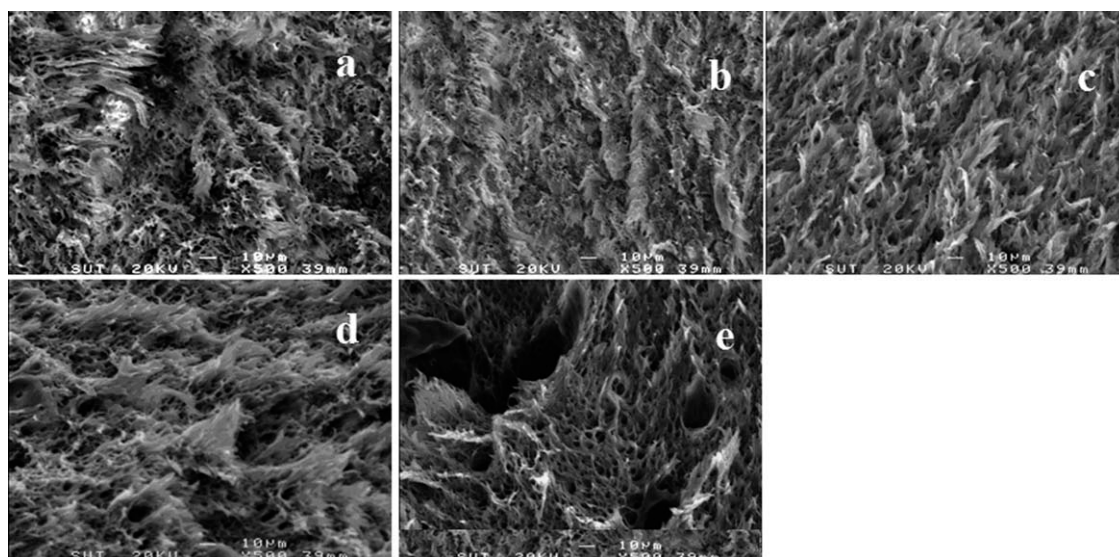


**Figure 12** SEM micrographs of tensile fractured surface of PLA/NR (90/10) (a), PLA/NR/NR-g-GMA (A) (90/9/1) (b), PLA/NR/NR-g-GMA (B) (90/9/1) (c), PLA/NR/NR-g-GMA (C) (90/9/1) (d), and PLA/NR/NR-g-GMA (D) (90/9/1) (e).



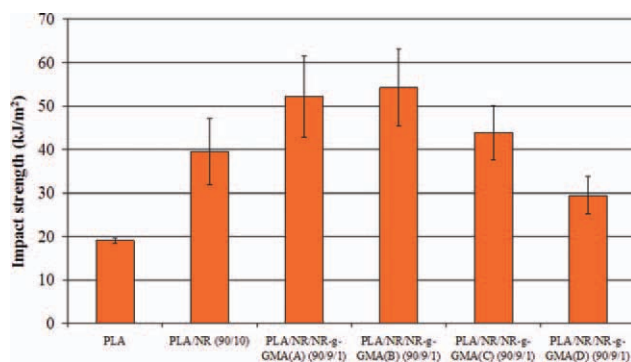


**Figure 13** Impact strength of PLA, PLA/NR (90/10) and PLA/NR/NR-g-GMA at various % grafting of NR-g-GMA. [Color figure can be viewed in the online issue, which is available at [wileyonlinelibrary.com](http://wileyonlinelibrary.com).]

blends was increased to 54.24 kJ/m<sup>2</sup> with increasing % grafting of NR-g-GMA to 4.35. When % grafting of NR-g-GMA was increased to 8.4, impact strength was decreased to 43.89 kJ/m<sup>2</sup>. This value was still higher than that of PLA/NR blend without NR-g-GMA. When % grafting of NR-g-GMA was increased to 16.7, impact strength was decreased to 29.46 kJ/m<sup>2</sup>. This value was much lower than that of PLA/NR blend without NR-g-GMA. The domain sizes of NR at high % grafting of NR-g-GMA were much larger than at low % grafting. In addition, poor distribution of NR particles can be observed. These caused the decrease in impact strength of PLA/NR/NR-g-GMA at high % grafting of NR-g-GMA. From this result, it can be suggested that NR-g-GMA exhibits compatibilization effect when using at low % grafting. Comparisons between mechanical properties of PLA, PLA/NR (90/10), and PLA/NR/NR-g-GMA at various % grafting of NR-g-GMA are shown in Table II. It was observed that elongation at break of PLA/NR blends increased to 159.08% for the blend containing NR-g-GMA with % grafting of 4.35 without significant loss in tensile strength and modulus. However, with increasing % grafting of NR-g-GMA in PLA/NR blend to 8.4 and 16.7, the elongation at break of the blend was decreased. This might be attributed to the large domain sizes of NR at high % grafting, which initiates the localized microdamages. As a consequence, the reduction of elongation at break at high % grafting of NR-g-GMA was observed.

## CONCLUSIONS

NR-g-GMA was shown to be an effective compatibilizer for PLA/NR blend. From FT-IR results, it was confirmed that the epoxy group in NR-g-GMA can react with the carboxyl groups of PLA chain ends during blending. This results in improved compati-

bility between PLA and NR. With the addition of NR-g-GMA, better dispersion and distribution of NR in PLA matrix can be observed by SEM micrographs. This led to a significant increase in impact strength and elongation at break without significantly loss in tensile strength and modulus of PLA/NR blend with NR-g-GMA. Moreover, an increase in thermal stability of PLA/NR when using NR-g-GMA as compatibilizer was observed. The effects of content and % grafting of NR-g-GMA on mechanical properties of PLA/NR blend were elucidated. With increasing NR-g-GMA content up to 1% (w/w), impact strength and elongation at break of PLA/NR blend increased about 2.5 times and 2 times, respectively. Moreover, with increasing % grafting of NR-g-GMA up to 4.35, the impact strength and elongation at break of PLA/NR/NR-g-GMA were increased.

The authors would like to send their sincere thank to Suranaree University of Technology and National Innovation Agency, Thailand for the financial support to this project.

## References

- Lunt, J. *Polym Degrad Stab* 1998, 59, 145.
- Broz, M. E.; Vanderhart, D. L.; Washburn, N. R. *Biomaterials* 2003, 24, 4181.
- Sarazin, P.; Li, G.; Orts, W. J.; Favis, B. D. *Polymer* 2008, 49, 599.
- Wu, D.; Zhang, Y.; Zhang, M.; Zhou, W. *Eur Polym J* 2008, 44, 2171.
- Yokohara, T.; Yamaguchi, M. *Eur Polym J* 2008, 44, 677.
- Shibata, M.; Inoue, Y.; Miyoshi, M. *Polymer* 2006, 47, 3557.
- Gu, S. Y.; Zhang, K.; Ren, J.; Zhan, H. *Carbohydr Polym* 2008, 74, 79.
- Long, J.; Michael, P. W.; Jinwen, Z. *Biomacromolecules* 2006, 7, 199.
- Mark, H. F. *Encyclopedia of Polymer Science and Engineering*; Wiley: New York, 1970. p 492.
- Phinyocheep, P.; Saelao, J.; Buzare, J. Y. *Polymer* 2007, 48, 5702.
- Asaletha, A.; Kumaran, M. G.; Thomus, S. *Eur Polym J* 1999, 35, 253.
- Oh, J. S.; Isayev, A. I.; Rogunova, M. A. *Polymer* 2003, 44, 2337.
- Carvalho, A. J. F.; Job, A. E.; Alves, N.; Curvelo, A. A. S.; Gandini, A. *Carbohydr Polym* 2003, 53, 95.
- Chuayjuljit, S.; Moolsin, S.; Potiyaraj, P. *J Appl Polym Sci* 2005, 95, 826.
- Carone, E. Jr; Kopcak, U.; Goncalves, M. C.; Nunes, S. P. *Polymer* 2000, 41, 5929.
- Dahlan, H. M.; Khairul Zaman, M. D.; Ibrahim, A. *Polym Test* 2002, 21, 905.
- Coltelli, M. B.; Bronco, S.; Chinea, C. *Polym Degrad Stab* 2010, 95, 332.
- Gao, Y.; Kong, L.; Zhang, L.; Gong, Y.; Chen, G.; Zhao, N.; Zhang, X. *Eur Polym J* 2006, 42, 764.
- Zhang, L.; Goh, S. H.; Lee, S. Y. *Polymer* 1998, 39, 4841.
- Wang, L.; Ma, W.; Gross, R. A.; McCarthy, S. P. *Polym Degrad Stab* 1998, 59, 161.

21. Huneault, M. A.; Li, H. *Polymer* 2007, 48, 270.
22. Chen, L., Qiu, X., Xie, Z., Hong, Z., Sun, J., Chen, X., Jing, X. *Carbohydr Polym* 2006, 65, 75.
23. Ho, C. H.; Wang, C. H.; Lin, C. I.; Lee, Y. D. *Polymer* 2008, 49, 3902.
24. Li, Y.; Shimizu, H. *Eur Polym J* 2009, 45, 738.
25. Su, Z.; Li, Q.; Liu, Y.; Hu, G. H.; Wu, C. *Eur Polym J* 2009, 45, 2428.
26. Oyama, H. T. *Polymer* 2009, 50, 747.
27. Pracella, M.; Chionna, D. *Macromol Symp* 2003, 198, 161.
28. Rosa, D. S.; Guedes, C. G. F.; Bardi, M. A. G. *Polym Test* 2007, 26, 209.
29. Pietrasanta, Y.; Robin, J. J.; Torres, N.; Boutevin, B. *Macromol Chem Phys* 1999, 200, 142.
30. Punmanee, J.; Chaiwat, R.; Praneee, C.; Yupaporn, R. *J Appl Polym Sci* 2011, 122, 3152.
31. Girija, B. G.; Sailaja, R. R. N.; Giridhar, M. *Polym Degrad Stab* 2005, 90, 147.
32. Feijoo, J. L.; Cabedo, L.; Gim, E.; Lagaron, J. M.; Saura, J. J. *J Mater Sci Lett* 2005, 40, 1785.
33. Chen, C. C.; Chueh, J. Y.; Tseng, H.; Huang, H. M.; Lee, S. Y. *Biomaterials* 2003, 24, 1167.
34. Todo, M.; Park, S. D.; Takayama, T.; Arakawa, K. *Eng Fract Mech* 2007, 74, 1872.